8-7-2017

Mechanistic Insight into Nanoparticle Surface Adsorption by Solution NMR Spectroscopy in an Aqueous Gel

Timothy K. Egner
Iowa State University, tkegner@iastate.edu

Pranjali Naik
Iowa State University and Ames Laboratory, naikpj@iastate.edu

Nicholas C. Nelson
Iowa State University and Ames Laboratory

Igor I. Slowing
Iowa State University and Ames Laboratory, islowing@iastate.edu

Vincenzo Venditti
Iowa State University, venditti@iastate.edu

Mechanistic Insight into Nanoparticle Surface Adsorption by Solution NMR Spectroscopy in an Aqueous Gel

Abstract

Engineering nanoparticle (NP) functions at the molecular level requires a detailed understanding of the dynamic processes occurring at the NP surface. Herein we show that a combination of dark-state exchange saturation transfer (DEST) and relaxation dispersion (RD) NMR experiments on gel-stabilized NP samples enables the accurate determination of the kinetics and thermodynamics of adsorption. We used the former approach to describe the interaction of cholic acid (CA) and phenol (PhOH) with ceria NPs with a diameter of approximately 200 nm. Whereas CA formed weak interactions with the NPs, PhOH was tightly bound to the NP surface. Interestingly, we found that the adsorption of PhOH proceeds via an intermediate, weakly bound state in which the small molecule has residual degrees of rotational diffusion. We believe the use of aqueous gels for stabilizing NP samples will increase the applicability of solution NMR methods to the characterization of nanomaterials.

Keywords

Adsorption, Desorption, Nanopartikel, NMR-unsichtbare Zustände, Oberflächenanalyse

Comments

This is the peer reviewed version of the following article: Egner, Timothy K., Pranjali Naik, Nicholas C. Nelson, Igor I. Slowing, and Vincenzo Venditti. "Mechanistic Insight into Nanoparticle Surface Adsorption by Solution NMR Spectroscopy in an Aqueous Gel." *Angewandte Chemie* 129, no. 33 (2017): 9934-9938, which has been published in final form at DOI: 10.1002/ange.201704471. This article may be used for non-commercial purposes in accordance with Wiley Terms and Conditions for Use of Self-Archived Versions.

(a) **Experimental ^{1}H-DEST profiles measured at saturation fields of 150 (red) and 300 (black) Hz for two different preparations of the NMR sample containing 10 mM Ph, 1 wt % ceria and 1 wt % agarose. Data from sample 1 are shown as open circles. Data from sample 2 are shown as open triangles.**

Mechanistic Insights into Nanoparticle Surface Adsorption by Solution NMR Spectroscopy in an Aqueous Gel

Timothy K. Egner, Pranjali Naik, Nicholas C. Nelson, Igor I. Slowing, and Vincenzo Venditti*

Abstract: Engineering nanoparticle (NP) functions at molecular level requires a detailed understanding of the dynamic processes occurring at the NP surface. Here we show that the combined analysis of Dark state Exchange Saturation Transfer (DEST) and Relaxation Dispersion (RD) NMR experiments acquired on gel-stabilized samples of NP allows for accurate determination of the kinetics and thermodynamics of adsorption. We used the former approach to describe the interaction of cholic acid (CA) and phenol (PhOH) with ~200 nm ceria NP. We show that, while CA forms weak interactions with the NP, PhOH is tightly bound to the NP surface. Interestingly, we found that adsorption of PhOH proceeds through an intermediate, weakly bound state in which the small molecule has residual degrees of rotational diffusion. We believe the use of aqueous gels for stabilizing NP samples will increase the applicability of solution NMR methods to characterization of nanomaterials.

Nanoparticles (NP's) are central to several areas of nanoscience including optoelectronics,[1] sensing,[2] medicine,[3] and catalysis.[4] NP's are usually made by inorganic and/or organic materials and owe some of their unique properties to their high surface area to volume ratio that maximizes the probability of constructive encounters with their target ligands. As such, the final properties and ultimate application of a NP depend on its surface composition and morphology. Capping agents can be applied to the surface of a NP to increase its solubility and direct its targeting.[5] Surface functionalization with enzymes or other catalysts can be used to produce NP's for industrial or therapeutic applications.[6] Therefore, elucidating the interactions occurring at the NP surface is crucial to understand and engineer its function at molecular level.

Although Solid State NMR methods are routinely employed to gain structural insights into small molecule/NP systems,[7] kinetic and thermodynamic aspects of the interaction (i.e. rate constants and populations for the adsorption/desorption equilibrium) are difficult to obtain by such techniques. Thus, there is a critical need to develop new strategies to gain mechanistic insights into the processes occurring at the NP surface. Several solution NMR techniques have been developed to probe and characterize interactions between small, NMR-visible molecules and large, NMR-invisible systems. Among these, Dark state Exchange Saturation Transfer (DEST),[8] and Relaxation Dispersion (RD)[9] experiments are particularly attractive because they can provide kinetic, thermodynamic, structural, and dynamic information on the interaction.[10] The combined analysis of DEST and RD data acquired at multiple saturation field strengths (for DEST) and spectrometer frequencies (for RD) has been recently used to provide fundamental insights into the binding of small proteins to large molecular machines,[11] aggregates,[8a, 12], biological membranes[13] or nanoparticles.[14] When using these techniques, two conditions must apply in order to accurately detect and characterize the interaction: 1) the NMR-visible molecule has to exchange between the free and bound states on the µs-s timescale, and 2) the NMR-visible and NMR-invisible molecules have to stay homogeneously suspended in the NMR sample throughout the NMR data acquisition period.[10] While the first condition is often satisfied by NP-small molecule interactions, obtaining NP suspensions that remain stable and homogeneous for several hours is often a challenge that limits the applicability of solution NMR methods to the characterization of NP's.

Here, we show that a 1 wt % agarose gel can be employed to prevent NP sedimentation and enable NMR characterization of adsorption/desorption kinetics of NMR-visible ligands to the surface of NMR-invisible NP's. The ability of agarose to provide a chemical inert matrix for studying ligand adsorption is tested by investigating the interaction between cerium oxide (ceria) NP's and two small molecules with different size and chemical properties: phenol (PhOH) and cholic acid (CA) (Supporting Information, SI, Figure S1). The study was conducted using NP's of cubic morphology and ~200 nm in size (SI, Figure S2). Ceria NP's were recently shown to actively participate in the Pd catalyzed hydrogenation of PhOH by 1) co-adsorbing the small molecule and the metal on the NP surface, 2) activating the PhOH molecule for the hydrogenation reaction, and 3) possibly participating in the electron transfer process during catalysis.[6b]

Addition of 1 wt % ceria to 10 mM PhOH or CA resulted in extensive line-broadening of the NMR resonances of the small molecules (Figure 1b), indicating that PhOH and CA interact with ceria and exchange between a free and NP-bound state. However, sedimentation of ceria caused a progressive reduction of the amount of NP in the NMR active volume (Figure 1a). This local change in the small molecule/NP ratio effectively reduces the fraction of small molecule bound to the NP that is detected by the NMR experiment, and results in a progressive shift of the small molecule NMR spectrum toward the free state (Figure 1b).

[a] Dr., V. Venditti, Mr. T.K. Egner, Ms. P. Naik, Dr. N.C. Nelson, Dr. I.I Slowing
Department of Chemistry
Iowa State University
2438 Pammel Dr., Ames, IA 50011 (USA)
E-mail: Venditti @iastate.edu
[b] Ms. P. Naik, Dr. N.C. Nelson, Dr. I.I Slowing
U.S. Department of Energy, Ames Laboratory
2756 Gilman Hall, Ames, IA 50011 (USA)

Supporting information for this article is given via a link at the end of the document.

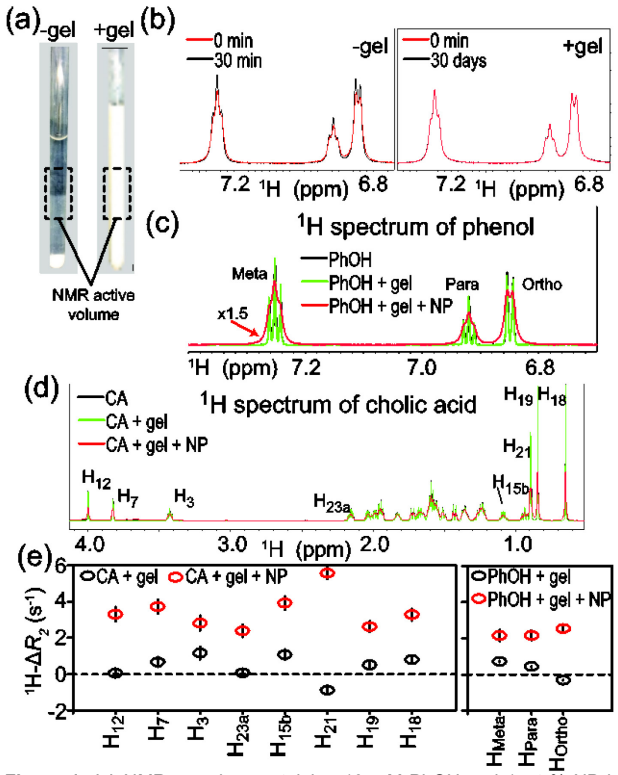

Figure 1. (a) NMR samples containing 10 mM PhOH and 1 wt % NP in the absence (left) and in the presence (right) of the gel matrix. Pictures were taken after one week and 6 months from sample preparation, respectively. **(b)** ^{1}H-NMR spectra of PhOH in the presence of 1 wt % NP were acquired 0 (red) and 30 (black) minutes after sample preparation. Samples were prepared in the absence (left) and in the presence (right) of the agarose gel matrix. ^{1}H-NMR spectra of **(c)** PhOH and **(d)** CA in the absence of gel (black), in the presence of the gel matrix (green) and in the presence of the gel matrix and 1 wt % NP (red). The spectrum acquired for PhOH in the presence of agarose and NP is multiplied by 1.5 in the figure. NMR signals used for the analysis of ^{1}H-DEST and ^{1}H-RD profiles are labeled according to the numbering scheme reported in SI, Figure S1. **(e)** Increase in ^{1}H-R_2 rate (ΔR_2) upon addition of the agarose gel matrix ($\boldsymbol{\Delta R_2^{gel}}$, black circles) and of the agarose gel matrix and 1 wt % NP ($\boldsymbol{\Delta R_2^{NP}}$, red circles) to 10 mM CA (left) and PhOH (right).

The rate of sedimentation depends strongly on sample conditions. Indeed, the presence of moderate amounts (≥ 20 mM) of buffer (Tris-HCl, or phosphate at pH 7.4) and/or NaCl resulted in complete sedimentation of ceria in less than 30 minutes at room temperature. Samples prepared in the absence of buffer and salts are more stable: complete ceria sedimentation is achieved after ~1 hour or ~1 week when 1 wt % NP is added to 10 mM CA (final pH = 10.0) or PhOH (final pH = 7.0), respectively. However, even in the case of the PhOH sample, for which NP sedimentation can be detected by visual inspection only after 2 days, the effects of sedimentation on the NMR spectra manifest on a much shorter time. Indeed, the data reported in Figure 1b show that ~15% increase in signal intensity is observed ~30 minutes after addition of NP to a 10 mM PhOH solution. Such dramatic change in spectral properties over time hampers acquisition of extensive and consistent sets of DEST and RD data to study small molecule binding to ceria.

In order to limit NP sedimentation, we have prepared NMR samples containing 10 mM PhOH or CA and 1 wt % NP in a 1 wt % agarose gel matrix (SI, Methods). Having a pore distribution in the 100-500 nm range,[15] the gel matrix keeps the NP in suspension (Figure 1a), and allows acquisition of reproducible NMR spectra for more than 30 days (Figure 1b). In addition, very weak signals originating from the gel matrix are detected in 1D proton spectra (SI, Figure S3), which reduces the chance of signal overlap with the analyte of interest. Importantly, in the absence of NP, the gel matrix does not perturb the ^{1}H-NMR spectra of PhOH and CA (Figures 1c,d), and the ΔR_2^{gel} values, measured as the increase in transverse relaxation rate (R_2) caused by incorporating the small molecules in the agarose gel ($\Delta R_2^{gel} = R_2^{gel} - R_2^{water}$), ~ 0 for all the analyzed NMR signals (Figure 1e). These findings indicate the absence of interactions between the investigated small molecules and the gel matrix. On the other hand, ΔR_2^{NP} values (i.e. the increase in R_2 caused by adding NP to the small molecule in the gel matrix; $R_2^{gel+NP} - R_2^{gel}$) larger than 0 were measured for small molecule samples prepared with 1 wt % agarose and 1 wt % NP (Figure 1e), which reflects the interaction of PhOH and CA with the large and slowly tumbling NP. Addressing whether the gel matrix affects the binding properties of the NP surface is an important, but not trivial task. Indeed, in the absence of agarose, the fast sedimentation of ceria does not permit to accurately describe the binding of CA and PhOH to the NP surface. However, for the PhOH/NP system (for which NP sedimentation in the absence of the gel matrix is slow), we observe very good agreement between ^{1}H-DEST data collected in the absence and in the presence of agarose within ~60 minutes from sample preparation (SI, Figure S4). This finding suggests that the NP surface displays similar PhOH binding properties when in water or suspended into the gel matrix.

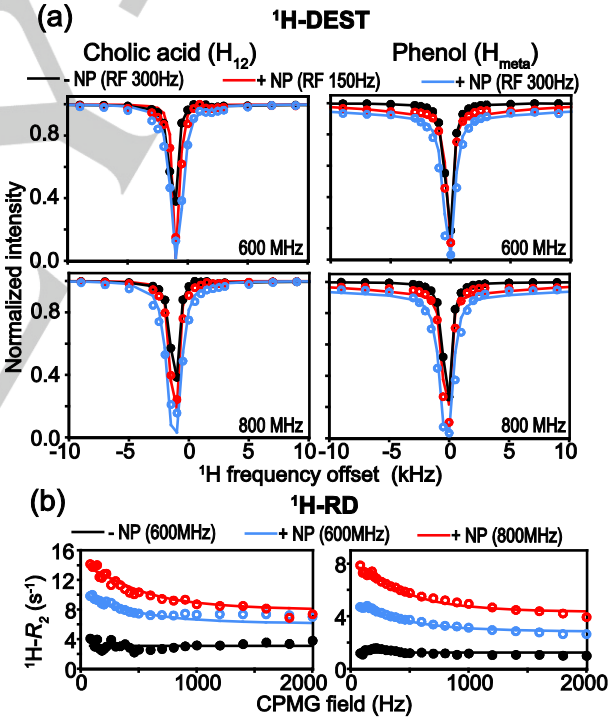

Figure 2. (a) ^{1}H-DEST profiles for H_{12} and H_{meta} positions of CA (left) and PhOH (right), respectively. Data were acquired on 800 (top) and 600 (bottom) MHz spectrometers. Experimental data are shown as circles. DEST profiles simulated from the best fit parameters (see main text) are shown as solid lines. Color code: 0 wt % NP and 300 Hz saturation field, black; 1 wt % NP and 150 Hz saturation field, red; 1 wt % NP and 300 Hz saturation field, blue. The complete set of ^{1}H-DEST profiles is shown in SI, Figures S5 and S6. **(b)** ^{1}H-RD profiles for H_{12} and H_{meta} positions of CA (left) and PhOH (right), respectively. Experimental data are shown as circles. RD profiles simulated from the best fit parameters (see main text) are shown as solid lines. Color code: 0 wt % NP and 600 MHz spectrometer, black; 1 wt % NP and 600 MHz spectrometer, blue; 1 wt % NP and 800 MHz spectrometer, red. The complete set of ^{1}H-RD profiles is shown in SI, Figures S7 and S8.

Binding of PhOH and CA to the surface of ceria NP's was investigated by ^{1}H-DEST and ^{1}H-RD experiments. Figure 2a shows examples of DEST profiles measured for the NMR signals of H_{12} and H_{meta} of CA and PhOH, respectively, at different spectrometer frequency (600 and 800 MHz) and different saturation field strength (150 and 300 Hz). The full set of DEST data is shown in SI (Figures S5 and S6). Addition of NP to CA and PhOH samples results in a broadening of the DEST profiles (Figure 2a), indicating the presence of high molecular weight small molecule-NP adducts in exchange with the free ligands. Interestingly, only a small increase in the width of the DEST profile is observed for CA upon addition of ceria, suggesting that this molecule interacts weakly with the NP. On the contrary, the very broad "wings" in the DEST profiles measured for PhOH (SI, Figure S6) suggests that the association of PhOH with the NP has a much longer lifetime.[8a, 12]

The existence of small molecule-NP interactions was confirmed by ^{1}H-RD experiments (Figure 2b and SI, Figures S7 and S8) acquired using a modified Carr-Purcell-Meinboom-Gill (CPMG) scheme that suppresses modulations from scalar couplings.[16] If a small molecule is in exchange on the µs-ms timescale between the free state (characterized by small R_2) and the NP-bound state (characterized by large R_2), and the free and bound states have different proton chemical shifts, the shape of the ^{1}H-RD profiles (Figure 2b) measured for the small molecule NMR signals will be affected by the exchange. At high CPMG field, the observed R_2 rate will be enhanced by lifetime line broadening ($R_2^{obs} = R_2^{free} + R_{llb}$, where R_2^{free} is the R_2 in the absence of NP and R_{llb} is lifetime line broadening).[10] At low CPMG fields, the observed R_2 rate will be enhanced by both lifetime line broadening and chemical exchange contribution to R_2 ($R_2^{obs} = R_2^{free} + R_{llb} + R_{ex}$, where R_{ex} is the exchange contribution to the relaxation rate).[10] Increasing the CPMG field results in a progressive suppression of R_{ex} and a decrease in R_2 (which value levels off when R_{ex} is fully suppressed by the CPMG field) that introduce a curvature (dispersion) in the RD profile. In the absence of NP, the R_2 rates measured for CA and PhOH are independent of the CPMG field (Figure 2b), consistent with the absence of small molecule-NP interactions. Conversely, samples prepared in the presence of 1 wt % NP display clear relaxation dispersion (i.e. $R_{ex} > 0$) and $R_{llb} > 0$ (i.e. R_2 at high CPMG filed is higher for the NP containing sample).

The data from the ^{1}H-DEST and ^{1}H-RD experiments were analyzed simultaneously using a two- or three-site exchange model (Figure 3) in which all the experimental observables are described by solutions to the McConnell equations (SI, Methods).[10, 17] For each small molecule, global nonlinear least-square fitting was carried out by optimizing the values of two (p_F, k_{RF}) and five (p_F, p_R, k_{RF}, k_{BR}, k_{BF}) global parameters for the two- and three-site exchange, respectively (Figure 3). Proton R_2 rates and chemical shift changes upon binding (Δ) were treated as peak-specific parameters. The best-fit parameters are reported in Tables S1 and S2 (SI) for CA and PhOH, respectively, and are summarized in Figure 3. The agreement between the experimental and back calculated DEST and RD profiles is shown in Figures 2 and S5-S8 (SI). CA binding to ceria is fully described by a two-site exchange model involving the free state (population, p_F, ~ 96 %, and average R_2 ~ 3 s^{-1}) and a NP-associated state with population ~ 4 % and average R_2 ~ 60 s^{-1}. Using the Stoke's law and approximating the NP to a sphere of 100 nm radius, an effective correlation time ($\tau_{eff} = 1/[1/\tau_c + k_{FR}^{app} + k_{RF}]$,[13b] where τ_c is the correlation time of the NP) of ~150 µs can be calculated in water at 25°C for a rigid CA-NP adduct, which would translate into an R_2 in the tens of thousands s^{-1} for a pair of isolated ^{1}H nuclei located 2.5 Å apart that undergo dipolar relaxation. The fact that CA in the NP-associated state has an R_2 that is three orders of magnitude smaller than the R_2 simulated for a rigid CA-NP adduct indicates that residual degrees of rotational diffusion increase the mobility of the small molecule associated to the NP surface, therefore decreasing its τ_{eff}. In this weakly associated state, CA does not form a rigid adduct with the NP, but its rotational diffusion is only marginally restricted compared to the free state (Figure 3). We refer to such "dynamic" small molecule-NP association as the "restricted state", as opposed to a rigidly bound species. The ζ-potential measured for the NP at pH 10.0 (corresponding to the pH of the NMR sample containing CA and NP) is -1.6 (SI, Methods), suggesting that formation of the restricted state is likely driven by hydrophobic and/or hydrogen-bonding interactions between CA and the NP surface.

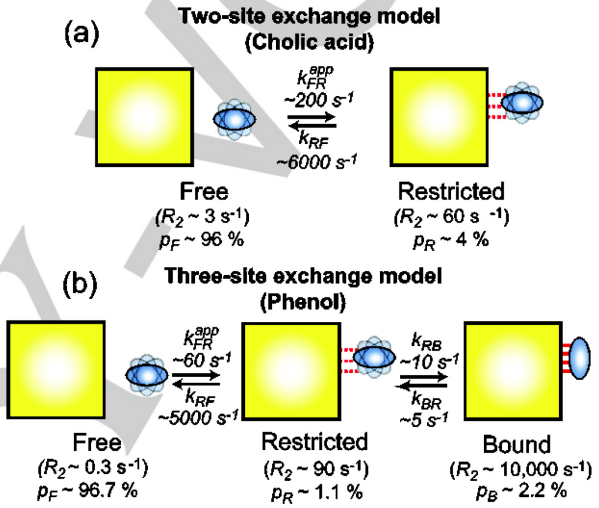

Figure 3. (a) The ^{1}H-DEST and ^{1}H-RD data measured for CA in the presence of 1 wt % NP are interpreted using a two-site exchange model. The NP-associated state forms weak interaction with ceria (see main text) and is referred to as "restricted state". **(b)** The ^{1}H-DEST and ^{1}H-RD data measured for PhOH in the presence of 1 wt % NP are interpreted using a three-site exchange model. The NP-associated state exists as a combination of restricted and bound states (see main text). The NP is represented as a yellow square. The small molecule is shown as blue oblate ellipsoid. Transparent blue oblate ellipsoids are used to indicate rotational diffusion of the small molecule. Solid and dashed red lines represent strong and weak interactions, respectively. Rate constants for each equilibrium (k_{xy}, where *x* and *y* are the states in thermodynamic equilibrium; k_{xy}^{app} indicates the apparent rate constant) and populations of each state (p_F, p_R and p_B for the free, restricted and bound states, respectively) were fit as global parameters. R_2 rates for each state and chemical shift changes associated with each equilibrium were fit as peak specific parameters (see SI, Methods). Best fit parameters are shown. For the R_2 rate of each state, the average over the analyzed NMR peaks is reported. The fit reveals that the free and bound states of PhOH are not kinetically connected ($k_{FB}^{app} = k_{BF} = 0$). A full report of the fitted parameters is shown in SI, Tables S1 and S2 for CA and PhOH, respectively. Results for the individual, atom-based fits of the ^{1}H-DEST and ^{1}H-RD data are shown in Figure SX (SI).

^{1}H-DEST data acquired for PhOH in the presence of 1 wt % NP cannot be fit using the two-site exchange model employed for CA (SI, Figures S6), but a three-site exchange has to be invoked in order to fully account for the experimental DEST and RD profiles (Figure 2 and SI, Figures S6 and S8). The three states have average R_2's of ~0.3, ~90, and ~10,000 s^{-1}, and represent the free, restricted and rigidly bound states, respectively (Figure 3 and SI, Table S2). Interestingly, the analysis of the DEST and RD data reveals that there is no direct communication between the free and rigidly bound states (i.e. $k_{FB}^{app} = k_{BF} = 0$; SI, Table S2), and that the restricted state is a weakly associated

intermediate on the pathway describing PhOH binding to ceria. Given the neutral electric charge of the NP surface at pH 7.0 (ζ-potential ~ 1.7 mV – SI, Methods), formation of the restricted state is likely driven by hydrophobic and/or hydrogen-bonding interactions between PhOH and NP. On the other hand, the tightly bound state might be the result of the interaction of the phenolic oxygen with a cerium atom from the NP surface.[6b] Establishment of this rigidly associated PhOH/NP adduct mediates PhOH activation and is an essential step in PhOH hydrogenation catalyzed by Pd supported on ceria NP.[6b] However, assessment of the role played by the equilibrium between the restricted and rigidly bound state in heterogeneous catalytic hydrogenation of PhOH is beyond the scope of the present work and will be the subject of future investigations.

In summary, we have shown that preparing nanoparticle samples in aqueous gels is a convenient strategy to avoid nanoparticle sedimentation for extended periods of time (up to several months), and allows acquisition of extensive sets of solution NMR experiments for investigating the thermodynamics and kinetics of binding to a NP surface. Interestingly, using this approach we have detected a motionally restricted intermediate state in PhOH binding to ceria NP, demonstrating that the method is capable to provide detailed mechanistic insights into surface adsorption processes. Agarose seems an ideal choice as the gel matrix since it is easy to prepare and does not introduce additional NMR signals. Most importantly, our data indicate that the agarose gel is an inert matrix that does not have detectable interactions with organic compounds (i.e. CA and PhOH) or proteins (i.e. ubiquitin; SI, Figure S10), and does not perturb small molecule binding to the surface of the ceria NP tested in this study. Preparation of homogeneous and stable samples is crucial for highly quantitative NMR measurements, especially for insensitive experiments that require extensive signal averaging (i.e. NMR experiments involving nuclei with low gyromagnetic ratio). We expect the use of aqueous gels to expand considerably the portfolio of NMR methods applicable to the characterization of NP's in solution, and to become a very valuable tool in understanding and guiding NP engineering.

Acknowledgements

We thank Vitali Tugarinov, Nick Fawzi and Aaron Rossini for helpful discussions. This work was supported by startup funding from Iowa State University (V.V.) and by the US Department of Energy, Office of Basic Energy Sciences, Division of Chemical Sciences, Geosciences, and Biosciences through the Ames Laboratory, operated by Iowa State University under Contract No. DE-AC02-07CH11358 (I.I.S., P.N., N.C.N.).

Keywords: Adsorption • Desorption • Nanoparticles • NMR Invisible states • Surface analysis

[[1] A. K. Podborska, M. F. Oszajca, S. A. Gaweda, K. T. Szacitowski, *IET Circuits, Devices & Systems* **2011**, *5*, 103-114.
[2] S. M. Ng, M. Koneswaran, R. Narayanaswamy, *RSC Advances* **2016**, *6*, 21624-21661.
[3] S. K. Murthy, *Int J Nanomedicine* **2007**, *2*, 129-141.
[4] Y. Xia, H. Yang, C. T. Campbell, *Acc Chem Res* **2013**, *46*, 1671-1672.
[5] aB. I. Kharisov, H. V. R. Dias, O. V. Kharissova, A. Vazquez, Y. Pena, I. Gomez, *RCS Adv* **2014**, *4*, 45354-45381; bS. Liang, Q. Zhou, M. Wang, Y. Zhu, Q. Wu, X. Yang, *Int J Nanomedicine* **2015**, *10*, 2325-2333; cO. Veiseh, J. W. Gunn, M. Zhang, *Adv Drug Deliv Rev* **2010**, *62*, 284-304.
[6] aR. T. Hill, J. B. Shear, *Anal Chem* **2006**, *78*, 7022-7026; bN. C. Nelson, J. S. Manzano, A. D. Sadow, S. H. Overbury, I. I. Slowing, *ACS Catalysis* **2015**, *5*, 2051-2061; cK. E. Sapsford, W. R. Algar, L. Berti, K. B. Gemmill, B. J. Casey, E. Oh, M. H. Stewart, I. L. Medintz, *Chem Rev* **2013**, *113*, 1904-2074.
[7] aT. M. Alam, J. E. Jenkins, in *Advanced Aspects of Spectroscopy* (Ed.: M. A. Farrukh), INTECH, **2012**, pp. 279-306; bT. Blasco, *Chem Soc Rev* **2010**, *39*, 4685-4702.
[8] aN. L. Fawzi, J. Ying, D. A. Torchia, G. M. Clore, *J Am Chem Soc* **2010**, *132*, 9948-9951; bN. L. Fawzi, J. Ying, D. A. Torchia, G. M. Clore, *Nat Protoc* **2012**, *7*, 1523-1533.
[9] F. A. Mulder, N. R. Skrynnikov, B. Hon, F. W. Dahlquist, L. E. Kay, *J Am Chem Soc* **2001**, *123*, 967-975.
[10] N. J. Anthis, G. M. Clore, *Q Rev Biophys* **2015**, *48*, 35-116.
[11] aD. S. Libich, N. L. Fawzi, J. Ying, G. M. Clore, *Proc Natl Acad Sci U S A* **2013**, *110*, 11361-11366; bD. S. Libich, V. Tugarinov, G. M. Clore, *Proc Natl Acad Sci U S A* **2015**, *112*, 8817-8823.
[12] N. L. Fawzi, J. Ying, R. Ghirlando, D. A. Torchia, G. M. Clore, *Nature* **2011**, *480*, 268-272.
[13] aG. Fusco, T. Pape, A. D. Stephens, P. Mahou, A. R. Costa, C. F. Kaminski, G. S. Kaminski Schierle, M. Vendruscolo, G. Veglia, C. M. Dobson, A. De Simone, *Nat Commun* **2016**, *7*, 12563; bA. Ceccon, V. Tugarinov, A. Bax, G. M. Clore, *J Am Chem Soc* **2016**, *138*, 5789-5792; cA. Ceccon, M. Lelli, M. D'Onofrio, H. Molinari, M. Assfalg, *J Am Chem Soc* **2014**, *136*, 13158-13161.
[14] aS. Zanzoni, A. Ceccon, M. Assfalg, R. K. Singh, D. Fushman, M. D'Onofrio, *Nanoscale* **2015**, *7*, 7197-7205; bS. Zanzoni, M. Pedroni, M. D'Onofrio, A. Speghini, M. Assfalg, *J Am Chem Soc* **2016**, *138*, 72-75.
[15] B. H. Zimm, S. D. Levene, *Q Rev Biophys* **1992**, *25*, 171-204.
[16] J. A. Aguilar, M. Nilsson, G. Bodenhausen, G. A. Morris, *Chem Commun (Camb)* **2012**, *48*, 811-813.
[17] M. Helgstrand, T. Hard, P. Allard, *J Biomol NMR* **2000**, *18*, 49-63.

Entry for the Table of Contents (Please choose one layout)

Layout 1:

COMMUNICATION

Solution NMR in an aqueous gel was used to investigate the kinetics and thermodynamics of small molecule adsorption on a nanoparticle surface. A multi-step binding mechanism is delineated in which a weakly associated encounter complex evolves into a tightly bound small molecule-nanoparticle adduct.

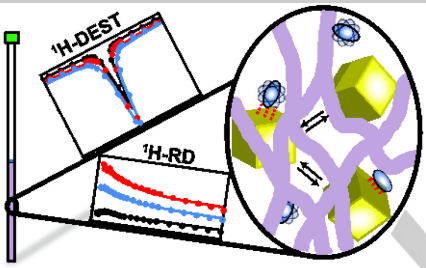

*Timothy K. Egner, Pranjali Naik, Nicholas C. Nelson, Igor I. Slowing, and Vincenzo Venditti**

Page No. – Page No.

Mechanistic Insights into Nanoparticle Surface Adsorption by Solution NMR Spectroscopy in an Aqueous Gel